IMPROVING 24-HOUR CLOUD FORECASTS BY MANUALLY-MODIFIED NUMERICAL PROGNOSES BASED ON SATELLITE OBSERVATIONS

Charlie Harvie Allen

NAVAL POSTGRADUATE SCHOOL
Monterey, California

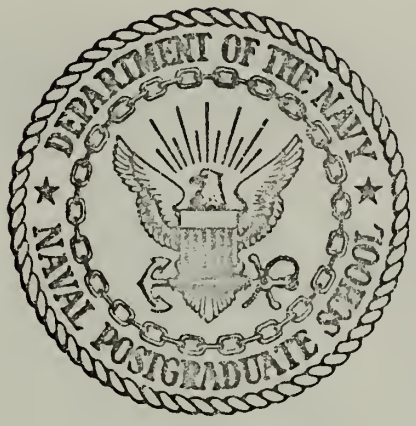

THESIS

IMPROVING 24-HOUR CLOUD FORECASTS BY
MANUALLY-MODIFIED NUMERICAL PROGNOSES
BASED ON SATELLITE OBSERVATIONS

by

Charlie Harvie Allen

Thesis Advisor: R. J. Renard

March 1973

Approved for public release; distribution unlimited.

Improving 24-Hour Cloud Forecasts By Manually-Modified Numerical Prognoses Based on Satellite Observations

by

Charlie Harvie Allen
Lieutenant, United States Navy
B.S., University of Oklahoma, 1965

Submitted in partial fulfillment of the
requirements for the degree of

MASTER OF SCIENCE IN METEOROLOGY

from the

NAVAL POSTGRADUATE SCHOOL
March 1973

ABSTRACT

The results of three quasi-objective techniques for enhancing the accuracy of 24-hour cloud cover forecasts in sparse data areas,using satellite data and numerically-produced analyses and prognoses, are presented. All three of the techniques involve the modification of the analyzed 500-mb relative vorticity, as based on the satellite-observed cloud patterns and the associated changes to the prognostic fields of 500-mb relative vorticity. The final 24-hour cloud-cover forecast is based on the manually-modified relative vorticity pattern and three different advecting currents. These advecting currents are based on the prognostic 500-mb height field, modified and unmodified, and the prognostic 500-mb space mean field. The study was conducted over a large area of the North Pacific Ocean for the period 9 March to 13 April 1972.

TABLE OF CONTENTS

LIST OF TABLES

LIST OF ILLUSTRATIONS

ACKNOWLEDGMENTS

The author wishes to express his gratitude to Commander Harry D. Hamilton, USN, for his technical advice and assistance during this thesis project. Even after his transfer to Fleet Numerical Weather Central, Monterey, California (FNWC), he continued to assist in every way possible, even though officially he had been assigned new duties. Dr. Robert J. Renard, who became the author's advisor upon the transfer of Commander Hamilton, was of invaluable help in the final stages of this project. Sincere thanks go to Professor van der Bijl for the time he spent working on the threat-score system which meant so much to the success of this project. My thanks also go to FNWC and the Environmental Prediction Research Facility, Monterey, California, who supplied the numerical and satellite data, respectively. Lastly, the author wishes to thank his wife who, although not a typist managed to type many copies of this work before the final draft was reached and who offered encouragement all along the way.

I. INTRODUCTION

The objective of this study was to investigate the possibility of increasing the accuracy of existing cloud cover forecasting techniques in sparse-data areas by using satellite data in conjunction with numerical analyses and prognoses. In particular, an improvement was sought on Bittner's [1] quasi-objective method of using the advection of relative vorticity on the 500-mb surface to determine the primary areas of cloud cover.

Bittner's quasi-objective method uses current satellite-observed cloud patterns to modify the analyzed patterns of relative vorticity. The difference between the initial and modified relative vorticity patterns is then subjectively applied to the 24- or 36-hour prognostic patterns of relative vorticity. The primary areas of cloud cover are then related to the areas of positive relative vorticity advection (PVA) as determined by the unmodified 24- or 36-hour prosnostic 500-mb height fields (Method 1).

Theoretically, an improvement in the cloud cover forecasts could be made if the prognostic 500-mb height fields were modified by the amounts associated with the changes in the prognostic relative vorticity fields prior to determining the areas of positive relative vorticity advection (Method 2).

Also, the theoretical development of Fjortoft [2] in manually producing a barotropic 24-hour forecast of the 500-mb height values indicates that using prognostic space-mean fields to determine the areas of positive relative vorticity advection might show an improvement in the verification of 24-hour cloud cover forecasts (Method 3).

Therefore, this study was specifically undertaken to determine which of the above three methods are the most accurate for forecasting 24-hour synoptic-scaled cloud patterns. All three techniques were used simultaneously to produce cloud-cover forecasts over the North Pacific Ocean from 20°N to 50°N and from 170°E to 125°W. The forecast period extended from 9 March to 13 April 1972.

Modifying the 500-mb height prognoses in addition to the relative vorticity prognoses took slightly longer than the other two methods, but the resultant improvement in the forecasts seemed to indicate that the small amount of additional work was well worth the effort involved.

II. BACKGROUND

The oceanic areas of the world are relatively void of conventional meteorological observations, especially above the earth's surface. Over the middle-latitude areas the synoptic-scaled cloud patterns attain their best development. Fortunately, these cloud patterns, which are so revealing of synoptic systems to trained meteorologists, are easily observed with satellites. Consequently, for the past several years, meteorologists have striven to incorporate the vast quantity of synoptic-scaled information obtained from satellites into useful models for improved forecasts. Further, there has been considerable effort to incorporate this satellite-derived data into numerical analysis schemes, as Nagle and Hayden[7], Nagle and Clark [6], Mantei and Workman [5], Zeigler (8] and Glaes [3]. Recently Bittner [1] has illustrated a method of using these satellite-observed synoptic-scaled cloud patterns to manually improve the numerical analysis of the 500-mb relative vorticity field. He then carried this improvement forward 24 to 36 hours by manually adjusting the numerically-produced prognostic 500-mb relative vorticity field. Finally, he converted this modified prognostic field into cloud and precipitation forecasts.

In an equivalent barotropic numerical model of the atmosphere it may be easily shown that the sign of the

advection of relative vorticity at the level of nondivergence (LND) is the same as the sign of the vertical motion through this level. In fact, in this simple model of the atmosphere the sign of the vertical motion is the same throughout a given column of air, if terrain effects are neglected. Therefore, positive advection of relative vorticity at the LND produces positive (upward) vertical motion throughout the column of air. In the real atmosphere the sign of the advection of relative vorticity, or geostrophic relative vorticity, on the 500-mb pressure surface is highly correlated with the sign of the synoptic-scaled vertical motion through this surface. That is, if the advection of geostrophic relative vorticity on the 500-mb surface is negative then the synoptic-scaled vertical motion in the vicinity of the 500-mb level is also negative (i.e. subsidence) almost all of the time.

If hygroscopic nuclei and moisture are present within the atmosphere then the formation and dissipation of clouds are largely determined by the sign of the vertical motion. That is, with the above conditions, positive vertical motion on a synoptic scale will produce synoptic-scaled cloud patterns when the time scale is sufficient to cover the phase lag between initial lifting and subsequent condensation. With a given moisture distribution, the stronger the advection of vorticity the shorter the time lag between the vertical ascent and its tell-tale signature, the synoptic-scaled cloud patterns.

For a given analysis or prognosis of the height field of a constant pressure surface the relative vorticity may be obtained diagnostically from an equation which relates the mass field to the wind field. The exact form of this diagnostic equation depends upon the assumptions made concerning the relationship between the wind field and the mass field. Fjortoft [2] demonstrated that the height field of a constant pressure surface may be smoothed by using a space differential operator called the Laplacian or del-squared operator. This smoothed height field is more commonly known in meteorology as the space mean. The space mean represents the initial height field after the shorter wave lengths have been selectively removed. The exact short wave length which is completely removed from this field depends upon the grid length selected for the finite difference equation used in the approximation of the analytical equation. Fjortoft proved that, except for a latitude-dependent weighting function, the geostrophic relative vorticity field is obtained when the initial height field is subtracted from this space-mean height field.

The height field of a constant pressure surface which is obtained through numerical analysis or prognosis may be subjected to the scale separation technique of Holl [4]. In effect the initial height field is repeatedly smoothed with a Laplacian operator until a residual field called

the SR field remains. This SR field may be roughly construed to be equivalent to the space-mean field described above. When this SR field is subtracted from the initial height only a disturbance field, called an SD field, remains. The SD field roughly represents the combined effect of all the numerically representable short waves with wave lengths shorter than wave number six. Likewise the SR pattern approximately depicts wave numbers zero (polar vortex) through six. Note that the field which approximates the geostrophic relative vorticity is the space-mean minus the initial height field while the SD field is minus the SR (space mean) plus the initial height field. That is, when the pattern of the SD analysis is used to approximate the pattern of the geostrophic relative vorticity, the sign of the SD centers must be reversed. See Appendix A.

Consequently, the above concepts led to the development of quasi-objective rules for relating synoptic-scale clouds to the 500-mb SD field. Bittner [1] outlined these and for convenience they are listed in Appendix B. Bittner's method consists of using the most recent satellite-observed cloud patterns to modify the current 500-mb SD analysis. The resulting difference field between the initial and modified SD patterns is applied to the prognostic SD field to produce modified forecast SD patterns.

The particular step of modifying the SD patterns of the prognostic field based on the modifications applied to the

current SD patterns appears to be the most subjective of all the procedural steps of Bittner's method. If there is no energy transformation occurring between the short waves represented by the SD field and the long waves portrayed by the SR field during the period of the prognosis, then the modifications of the prognostic SD patterns are rather straight forward. However, for a given cyclonic or anticyclonic system within an initial SD field, the greater the forecast change of development of a short-wave feature the less reliable the modification which is applied to the SD system of the prognostic field. That is, the more an SD center changes during a prognostic period, the more difficult it becomes to propagate an initial modification of the SD center to its prognostic counterpart.

The modified SD prognosis is then used in conjunction with the unchanged 500-mb height prognosis to derive a subjective cloud and precipitation forecast valid at the time of the numerical height forecast. Bittner makes the following assumptions relative to his synoptic-scaled cloud pattern forecasts:

1) Large-scale vertical motion fields are highly correlated with the characteristic distribution of extratropical, synoptic-scale cloud patterns as seen by satellites.

2) In turn, the vertical motion patterns are closely related to the advection of relative vorticity at 500 mb.

3) An SD field is equivalent to a relative vorticity field. See Appendix A.

4) Any errors in the SD field based on the initial 500-mb analysis are propagated during the numerical prognosis to produce similar errors in the SD field based on the prognostic 500-mb heights. Hence the error field is assumed to be conserved during the prognosis.

III. DATA SOURCES AND SELECTION OF STUDY AREA AND PERIOD

An area of the North Pacific Ocean extending from 20°N to 50°N and from 170°E to 125°W was selected for investigation for several reasons.

This area was selected primarily because it is both analyzed numerically by FNWC and has almost continuous daylight picture coverage by the ATS-1 satellite. ATS-1 is the designator for the geostationary Applications Technology Satellite positioned near the equator of the Pacific Ocean since November 1967. Its spin-scan cloud camera takes time-lapse photographs approximately every 25 minutes. The resulting pictures cover a region from about 50°S to 50°N over a span of 100 degrees of longitude centered at 150°W, with a resolution of two miles at the center.

The subject ATS-1 photographs were generally available locally from FNWC on a real-time basis Monday through Friday. Since the Saturday photograph was needed for verification of Friday's forecast, the study period was usually limited to four days per week, namely Monday through Thursday. Some of these photographs and others that were missing on occasion were supplied by the Naval Air Systems Command's Project FAMOS.[1] The FNWC computer products were also available locally on a real-time basis.

---

[1]Presently part of the Environmental Prediction Research Facility, Monterey, California.

The period selected (March and April 1972) not only afforded a real-time basis for investigation but it is also the time of year when large, well-defined systems characterize the North Pacific Ocean. These systems readily lend themselves to the modification techniques evaluated during this study.

IV. PROCEDURES

The research objectives of the procedures described below were to extend Bittner's work [1] and to outline an approach which would be practical for Fleet use. At the time when the FNWC 0000 GMT numerical analyses are received by the Weather Centrals and Facilities, the prognostic fields are not yet available. Therefore, to expedite 24-hour cloud forecasts from 0000 GMT it would be best to use the 36-hour prognostic height fields, as based on the previous 12-hour analysis, and the current 0000 GMT analysis. Bittner indicated his approach is good for 24- and 36-hour forecasts. Since he effectively assumes that there is no energy transformation occurring between the SD and SR fields for 24 to 36 hours, then a change in an SD pattern may be propagated forward from any time step within this forecast period. That is, a change in the SD pattern at plus 12 hours from the time of the forecast may be carried forward to plus 36 hours. Therefore, in these procedures, changes noted in the 0000 GMT analysis of the SD patterns were incorporated in the prognostic SD patterns which verified 24 hours later, but which were made from the previous 1200 GMT analysis.

Another point which may be mentioned in this regard is that within a sparse upper-air data area such as the North Pacific Ocean, the difference between the 12-hour prognosis

of the 500-mb level and the verifying 500-mb analysis may be quite small.

The procedures in this study deal almost exclusively with FNWC's scale separation products reproduced on a 1:60,000,000 polar stereographic projection. This required one scale change--that of manually transferring the cloud features of the ATS-1 photograph to this scale. FNWC is currently testing a program that will convert their products to the scale and projection of the ATS-1 photograph. When this is perfected, all future studies can be carried out on the ATS-1 scale to eliminate any errors in the manual transfer process.

In general, this study consisted of determining a modified SD field and projecting these modifications on the prognostic SD field. Then by using three advecting fields (FNWC's Z and SR PROGS, and a hand-modified FNWC Z PROG, called Z'PROG), three cloud cover forecasts were determined for verification. The detailed procedures are as follows:

1) Each day the ATS-1 photograph closest in time to 0000 GMT was selected for use. The major cloud features were traced onto a matching grid (same scale and subpoint as the photograph), carefully delineating as covered those areas with greater than 50% cloud cover and as open those areas with less than 50% coverage.

2) The cloud patterns were then transferred by hand to a polar-stereographic projection of 1:60,000,000 scale.

This was a difficult and tedious procedure at first but after some practice, the time was decreased to less than 15 minutes per map.

3) FNWC's SD and SR analyses were put in register with the transferred cloud patterns. In areas of major cloud features such as fronts, cyclones, etc., the SD patterns and isolines were modified in accordance with the rules specified by Bittner [1]. These rules are listed in Appendix B for convenience to the reader. Further, areas of greater than 50% cloud cover were assumed to be associated with positive vertical motion as indicated by positive vorticity advection using analyzed SR winds as the advecting field. The SD lines were redrawn to indicate the required advection in order to support the observed cloud patterns. Since the zero lines are not produced on the SD charts, these lines were drawn by hand. The result of the above was a modified SD chart, hereafter referred to as the SD' analysis. The SR fields were not modified.

4) Subjectively, the same adjustments that were made to the SD analysis were then applied to the 36-hour SD prognosis, hereafter designated as the SD' prognosis. Since the location of zero-valued SD isolines are somewhat arbitrary, care must be used to surround the same centers with the same zero line on both the analysis and the prognosis.

5) The SD' prognosis was then graphically added to the SR prognosis to produce a modified 500-mb height prognosis, hereafter indicated as a Z' prognosis.

6) The Z' prognosis was put in register with the SD' prognosis and used as the advecting field. Clouds were forecast in all areas of negative SD advection (positive relative vorticity advection). Clear skies (less than 50% covered) were forecast for areas of positive SD advection (negative relative vorticity advection). Note that clouds (greater than 50% covered) were assumed to be located only in areas of positive relative vorticity advection in this study. This is a slight deviation from Bittner's forecasting procedures for clouds as noted below.

7) To produce the second cloud cover forecast, steps 1) through 4) are the same but step 5)is omitted since the SR prognosis was used as the advection field for the purpose of step 6).

8) To construct the third cloud cover forecast, steps 1)through 4) are the same but step 5) is omitted since the unmodified Z prognosis was used as the advecting field (Bittner's approach [1]) for the purpose of step 6).

9) Steps 1) and 2) above were then applied to the next day's ATS-1 photograph (current plus 24 hours) to produce a verifying nephanalysis.

10) The verifying nephanalysis was separately put in register with the three forecasts. Each of the 351 grid points for each of the three forecasts was checked and compared with the corresponding grid point of the verifying nephanalysis. Grid points which were observed clear but forecast cloudy were denoted by a "2". Those which

were both forecast and observed cloudy were indicated with a "0". Next, the points which were observed cloudy but forecast clear were denoted by a "1". Finally the grid points which were not covered by clouds on the verifying nephanalysis nor forecast to be cloudy were represented by a "3". At this point the technique which gave the best results could be readily determined by totaling the number of correct forecasts ("0" and "3") for each forecast day. Tables I, II and III give the raw scores for the advecting fields of the Z' PROG, SR PROG and Z PROG, respectively. The sixth column represents the number of correct forecasts while the seventh column denotes the number of incorrect forecasts.

11) Finally, the National Meteorological Center's threat score was computed for each of the forecasts. An explanation of the threat score is presented in Section VI.

As indicated earlier, the manner in which the clouds were determined by this author is not strictly the same as that used by Bittner [1]. In addition, he applied the rules of Appendix B in reverse to indicate some geometric detail in the cloud patterns, as spiral clouds, vortices, etc., whenever they were deemed necessary as determined by the SD' prognosis. He also used various crossing-angle rules as a guide for forecast cloud tops, areas and amounts of precipitation, etc. Since this study was conducted to try and improve Bittner's basic premise, these refinements were not included.

TABLE I. Verification of grid-point cloud forecasts using the Z'PROG as the advecting field. (Tabular values are number of grid points.)

Verification Date/Time 1972 00 GMT	Clouds: FCST BUT NOT OBS "2"	Clouds: FCST AND OBS "0"	Clouds: OBS BUT NOT FCST "1"	Clear: FCST AND OBS "3"	Correct FCSTS = "0 + 3"	Incorrect FCSTS = "1 + 2"
3/10	59	135	48	109	244	107
3/15	40	121	132	58	179	172
3/16	51	130	74	96	226	125
3/17	52	108	94	97	205	146
3/22	56	84	116	95	179	172
3/23	60	113	64	114	227	124
3/24	55	162	82	52	214	137
3/25	50	151	83	67	218	133
4/1	39	169	62	81	250	101
4/4	41	168	101	41	209	142
4/5	24	202	104	21	223	128
4/6	43	188	98	22	210	141
4/7	38	250	41	22	272	79
4/8	61	207	42	41	248	103
4/9	39	173	61	78	251	100
4/10	57	178	66	50	228	123
4/11	65	141	101	43	184	166
4/12	66	165	93	27	192	159
4/13	52	122	103	74	196	155
4/14	72	78	134	67	145	206
Average					215	136

TABLE II. Verification of grid-point cloud forecasts using the SR PROG as the advecting field. (Tabular values are number of grid points.)

Verification Date/Time 1972 00 GMT	Clouds: FCST BUT NOT OBS "2"	Clouds: FCST AND OBS "0"	Clouds: OBS BUT NOT FCST "1"	Clear: FCST AND OBS "3"	Correct FCSTS = "0 + 3"	Incorrect FCSTS = "1 + 2"
3/10	60	134	52	105	239	112
3/15	44	110	142	55	165	186
3/16	57	138	68	88	226	125
3/17	46	114	95	96	210	141
3/22	57	86	112	96	182	169
3/23	59	110	63	119	229	122
3/24	53	140	106	52	192	159
3/25	35	140	106	70	210	141
4/1	45	145	73	88	233	118
4/4	37	157	114	43	200	151
4/5	24	174	132	21	195	156
4/6	42	160	122	27	187	164
4/7	44	237	50	20	257	94
4/8	71	198	47	35	233	118
4/9	41	173	60	77	250	101
4/10	71	161	79	40	201	150
4/11	76	135	105	35	170	181
4/12	63	172	88	28	200	151
4/13	52	118	102	79	197	154
4/14	76	73	134	68	141	210
Average					206	145

TABLE III. Verification of grid-point cloud forecasts using the Z PROG as the advecting field. (Tabular values are number of grid points.)

Verification Date/Time 1972 00 GMT	Clouds: FCST BUT NOT OBS "2"	Clouds: FCST AND OBS "0"	Clouds: OBS BUT NOT FCST "1"	Clear: FCST AND OBS "3"	Correct FCSTS = "0 + 3"	Incorrect FCSTS = "1 + 2"
3/10	62	121	65	103	224	127
3/15	45	108	145	53	161	190
3/16	49	130	80	92	222	129
3/17	40	112	97	102	214	137
3/22	55	74	120	102	176	175
3/23	60	107	68	116	223	128
3/24	52	145	99	55	200	151
3/25	45	139	99	68	207	144
4/1	49	147	82	73	220	131
4/4	42	165	110	34	199	152
4/5	25	197	106	23	220	131
4/6	35	176	111	29	205	146
4/7	44	230	55	22	252	99
4/8	45	183	66	57	240	111
4/9	44	164	71	72	236	115
4/10	76	148	90	37	185	166
4/11	74	127	110	40	167	184
4/12	58	166	92	35	201	150
4/13	53	105	115	78	183	168
4/14	77	78	126	70	148	203
Average					204	146

V. CASE STUDY OF MODIFICATIONS TO ANALYSES

The synoptic time of 0000 GMT 10 April 1972 and its associated analyses and prognoses were randomly selected as an example of the procedures presented in the preceding section. Figures 1 through 18 graphically illustrate the following discussion.

Figure 1 is the ATS-1 photograph of 2343 GMT 9 April 1972 which was selected to be representative of the cloud cover for 0000 GMT 10 April 1972. The major cloud features (areas of $\geq$ 50% cloud cover) are outlined for clarity.

In general, SD patterns moving into the western sector of the verification grid were modified very little because the cloud patterns are not well-defined near 170°E in the ATS-1 pictures. This sometimes led to a large error in the verification of cloud forecasts west of 180°. There was usually good definition of the cloud features and, therefore, accurate modifications of the SD patterns in the extreme eastern section of the grid. These eastern SD features and associated cloud features sometimes moved out of the area of the verification grid during the time-span of the prognosis. Some of the centers of the SD analyses in this near North American coastal area were extensively modified. For those systems which did not appear within the verification area at the verifying time

of the prognosis, the overall goodness of the associated modifications and the resultant cloud forecasts are unknown.

Figure 2 shows a nephanalysis (areas of $\geq$ 50% cloud cover as derived from Figure 1, on a grid of the same scale.

Figure 3 is the nephanalysis after it has been transferred to a polar stereographic projection with the SD and SR fields superimposed. The SD pattern is illustrated with dashed lines and the SR field with solid lines. Note the strong SD low center at 43°N and 135°W. Such a low value for the SD center suggests a cyclone at 500 mb. Since this center is embedded in an SR trough, as indicated by the solid lines, there is high probability of a closed center at 500 mb. However, the cloud patterns of Figure 1 indicate only slight cyclonic circulation with convective clouds in the area. This suggests decreasing the positive vorticity advection (negative SD advection) considerably.

Figure 4 shows the new or modified SD field. Note the drastic changes made to the SD zero line. In the lower left portion of the figure, the zero line was relocated to the poleward edge of the frontal cloud band. (Rule 1.a Appendix B). In general, SD troughs and ridges were redrawn to coincide with major cloud boundaries. Note the considerable filling of the SD low center at 43°N, 135°W to decrease the negative SD advection. The center at 33°N 180° was moved slightly northward to maintain the correct

perspective with the circulation center on the photograph. (See rule 2.e Appendix B.)

Figure 5 is the modified SD analysis of Figure 4 (dashed lines) superimposed on the original SD field of Figure 3 (solid lines). The amount and direction of movement of all centers and isolines were noted and used in the modification of the SD prognosis.

Figure 6 represents the 36-hour SD prognosis and its modification (SD' PROG). As such, it represents the changes made to the SD analysis 24 hours earlier, as shown in Figure 5. As can be seen from the figure, this modification is somewhat subjective.

Figure 7 shows the graphical addition of the modified SD prognosis (SD' PROG) to the SR prognosis in order to produce a new height prognosis (Z' PROG). This is the only additional step required over Bittner's method.

Figure 8 is the Z' prognosis of Figure 7 superimposed on the SD' prognosis of Figure 6. Since the negative SD values correspond to positive values of vorticity, as shown in Appendix A, the areas of positive vorticity advection (PVA) are readily apparent. These areas are carefully delineated and are represented in the figure as clouds. Note that major cloud boundaries are determined by the SD troughs and ridges as defined earlier relative to vorticity advection and as stressed by Bittner. As mentioned in the previous section, Bittner inserted cloud-pattern detail (i.e. cloud vortices, developing cyclones, etc.) at this

point. These modifications could be done by a knowledgeable synoptic meteorologist resulting in better continuity of cloud patterns and increased accuracy of cloud forecasts.

Figures 9 and 10 are the same as Figure 8 except that the vorticity-advection areas are determined by using the SR unmodified Z prognoses as the advection fields, respectively. See procedures 7 and 8 of the previous section.

Figure 11 is the verifying ATS-1 photograph with areas of $\geq$ 50% cloud cover outlined. This picture also shows very little cyclonic motion in the northeast corner, justifying the decreased PVA of Figure 4.

Figure 12 shows the boundaries of the $\geq$ 50% cloud cover from the photograph of Figure 11.

Figure 13 illustrates the verifying clouds as transferred from Figure 12 and the PVA areas derived in Figure 8 from the Z' prognosis. As mentioned earlier, the date for this case study was chosen at random; it just happens to be a below-average date. See Tables I, II and III for comparisons of raw values for 0000 GMT 11 April 1972.

Figure 14 represents the accuracy of the forecast. The 351 grid points of Figure 13 (every 2-1/2° latitude-longitude spacing) were examined and assigned to one of four categories. The grid points that were forecast to be cloudy but were observed to be clear ("2") totaled 65. Those that were both forecast and observed cloudy ("0") amounted to 141. Observed cloudy but forecast clear ("1")

were 101 points. And, finally, those grid points which were both forecast and observed to be clear ("3") totaled 43. This amounted to 184 correct ("0 + 3") and 166 ("1 + 2") incorrect forecasts, which yields a combined threat score[2] of .67. See discussion in Section VI and scores in Table IV.

Figures 15 and 16 show the verifying clouds superimposed on the PVA area derived from the SR prognosis and the scoring grid, respectively. The number of grid points with correct forecasts ("0 + 3") amounted to 170 while the incorrect total ("1 + 2") was 181. The threat score for this method was .59.

In general, the scores for all three methods in this case study were below their respective averages. See Table IV for the averages. However, the relative differences between the three methods are of the same order as the overall averages of each. That is the SR method of determining the PVA areas yielded approximately the same score as Bittner's technique (unmodified Z field) for determining PVA areas while the Z' (modified Z field) method gave better than a 10% increase in the value of the combined threat score which was used to evaluate the cloud cover forecasts.

---

[2]Threat score will be explained in detail in the following section.

VI. VERIFICATION OF RESULTS

The National Meteorological Center's threat score system was used to measure the goodness of the forecasts. The score depends on the correct forecasting of cloudy ($T_{\bullet}$) and clear areas (T_0). They are calculated as follows:

$$T_{\bullet} = \frac{0}{0+1+2} \quad \text{and} \quad T_0 = \frac{3}{3+1+2}$$

where:

0 = Those points both forecast and observed as cloudy.

1 = Those points forecast clear but observed as cloudy.

2 = Those points forecast cloudy but observed as clear.

3 = Those points both forecast and observed as clear.

Using this approach, a perfect forecast of clouds results in a score of $T_{\bullet} = 1.0$ and a perfect forecast of clear skies results in a score of $T_0 = 1.0$. Combining these two perfect threat scores gives a total of 2.0 for an absolutely correct forecast over an area as follows:

$$T_{\bullet} + T_0 = 1.0 + 1.0 = 2.0$$

The results of the three forecasts prepared for each day are listed in Table IV. These scores were obtained using the above technique. A cloudy forecast score and a clear forecast score followed by a combined score are

presented for each day of the study period. The overall averages of each method are listed at the bottom of the table.

The results of Bittner's study of approximately the same area of the North Pacific Ocean, but for different dates, are presented in Table V for comparison. The unmodified column represents threat scores obtained without the use of satellite pictures to modify either the initial or prognostic SD fields. The modified column represents the forecasts obtained after the initial SD fields have been modified based on the satellite observed cloud patterns and the prognostic SD fields have been modified based on the modifications applied to the initial SD patterns. This latter column represents a 15% increase in cloud-cover forecasting accuracy over the unmodified column. Except for the additional refinement steps mentioned earlier, this modified column is equivalent to the Z PROG column of Table IV. The additional refinements in forecasting cloud cover used by Bittner may account in large part for the relative accuracy differences between the two corresponding columns of Tables IV and V. However, as noted earlier, these refinements may be easily added to the basic approach in determining the PVA-associated cloud cover.

The basic determination of the PVA areas by the three different methods used in this study are clearly comparable.

The results in Table IV indicate that the Z PROG and the SR PROG advection fields are about equal in their results. The Z' PROG advection fields indicate about a 10% improvement over the approach suggested by Bittner [1]. Thus it may be argued that if Bittner's approach is modified to the extent of including the Z' (vice the Z) prognosis for the advecting field, before adding the required and obvious continuity of large-scale cloud patterns, the best 24-hour cloud-cover fields may be produced.

TABLE IV. A comparison of threat scores of Z'PROG, SR PROG and Z PROG cloud-cover forecasting techniques.

Verification DATE /Time	Z'PROG			SR PROG			Z PROG		
1972 00 GMT	$T_\odot$	+ T_0	= T	$T_\odot$	+ T_0	= T	$T_\odot$	+ T_0	= T
3/10	.95	.51	1.46	.54	.48	1.02	.49	.46	.95
3/15	.41	.25	.66	.37	.23	.60	.36	.22	.58
3/16	.51	.43	.94	.52	.41	.93	.50	.42	.92
3/17	.43	.40	.83	.44	.40	.84	.45	.43	.88
3/22	.33	.36	.69	.34	.36	.70	.30	.37	.67
3/23	.48	.48	.96	.47	.49	.96	.46	.48	.94
3/24	.54	.28	.82	.47	.25	.72	.50	.27	.77
3/25	.53	.34	.87	.50	.33	.83	.49	.32	.81
4/1	.67	.45	1.12	.55	.43	.98	.53	.36	.89
4/4	.41	.22	.63	.51	.22	.73	.52	.18	.70
4/5	.61	.14	.75	.53	.12	.65	.60	.15	.75
4/6	.57	.14	.71	.49	.14	.63	.55	.16	.71
4/7	.76	.22	.98	.72	.18	.90	.70	.18	.88
4/8	.67	.29	.96	.63	.23	.86	.62	.34	.96
4/9	.63	.44	1.07	.63	.43	1.06	.59	.38	.97
4/10	.59	.29	.88	.75	.21	.96	.47	.18	.65
4/11	.46	.21	.67	.43	.16	.59	.41	.18	.59
4/12	.89	.15	1.04	.53	.16	.69	.53	.19	.72
4/13	.44	.32	.76	.43	.34	.77	.38	.32	.70
4/14	.27	.24	.51	.26	.24	.50	.34	.25	.59
Average	.56	.31	.87	.51	.29	.80	.49	.29	.78

TABLE V. The results of Bittner's study [1].

DATE	UNMODIFIED			MODIFIED		
1969	T_e	+ T_0	= T	T_e	+ T_0	= T
10/3	.34	.66	1.00	.22	.61	.83
10/9	.30	.63	.93	.33	.73	1.06
10/10	.29	.49	.78	.34	.66	1.00
10/13	.24	.58	.82	.32	.66	.98
10/14	.14	.60	.74	.23	.63	.86
10/15	.28	.59	.87	.32	.68	1.00
10/16	.24	.57	.81	.34	.74	1.08
10/17	.35	.68	1.03	.26	.70	.96
10/18	.24	.57	.81	.36	.80	1.16
10/19	.45	.79	1.24	.40	.84	1.24
10/20	.27	.62	.89	.31	.68	.99
10/21	.32	.65	.97	.34	.71	1.05
10/24	.26	.43	.69	.25	.68	.93
10/25	.38	.61	.99	.27	.60	.87
10/27	.25	.60	.85	.43	.78	1.21
10/30	.26	.35	.61	.40	.63	1.03
11/4	.32	.57	.89	.28	.57	.85
Average	.29	.59	.88	.32	.69	1.01

VII. CONCLUSIONS

This study indicates there is merit in using the satellite-observed cloud patterns to modify the position and orientation of 500-mb relative vorticity patterns (the SD fields of FNWC) in order to improve 24-hour forecasts of cloud cover over oceanic areas. Bittner [1], in an earlier study, came to the same conclusion.

It appears that Bittner's basic approach can be improved by using both modified prognostic relative vorticity patterns and modified prognositic height fields at 500 mb. However, the refinements of cloud-pattern continuity described by Bittner should be included in the final 24-hour cloud pattern forecast for best results.

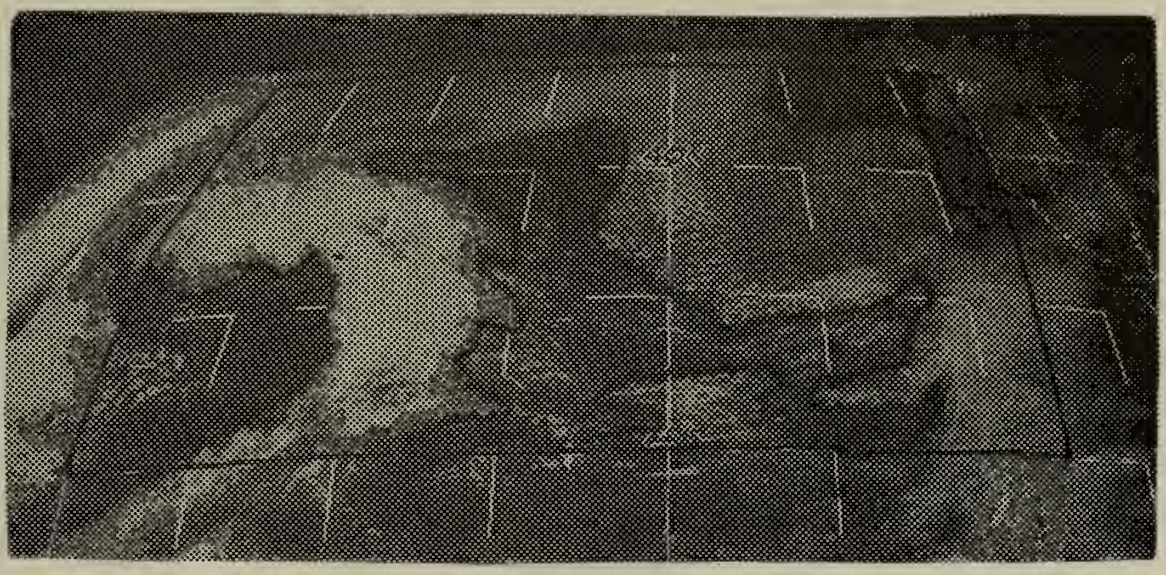

Figure 1. 2343 GMT 09 April 1972 ATS-1 satellite photograph (Subpoint: 2°S). Area of $\geq$ 50% cloud cover bounded by .

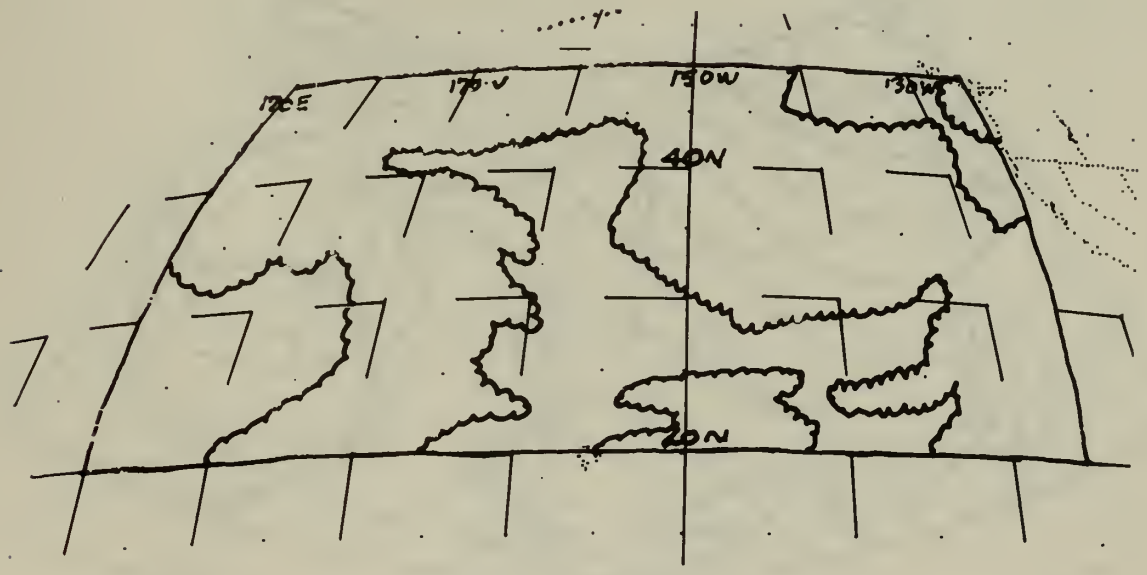

Figure 2. Nephanalysis of ATS-1 satellite photograph (Subpoint: 2°S), 2343 GMT 09 April 1972. Area of $\geq$ 50% cloud cover bounded by .

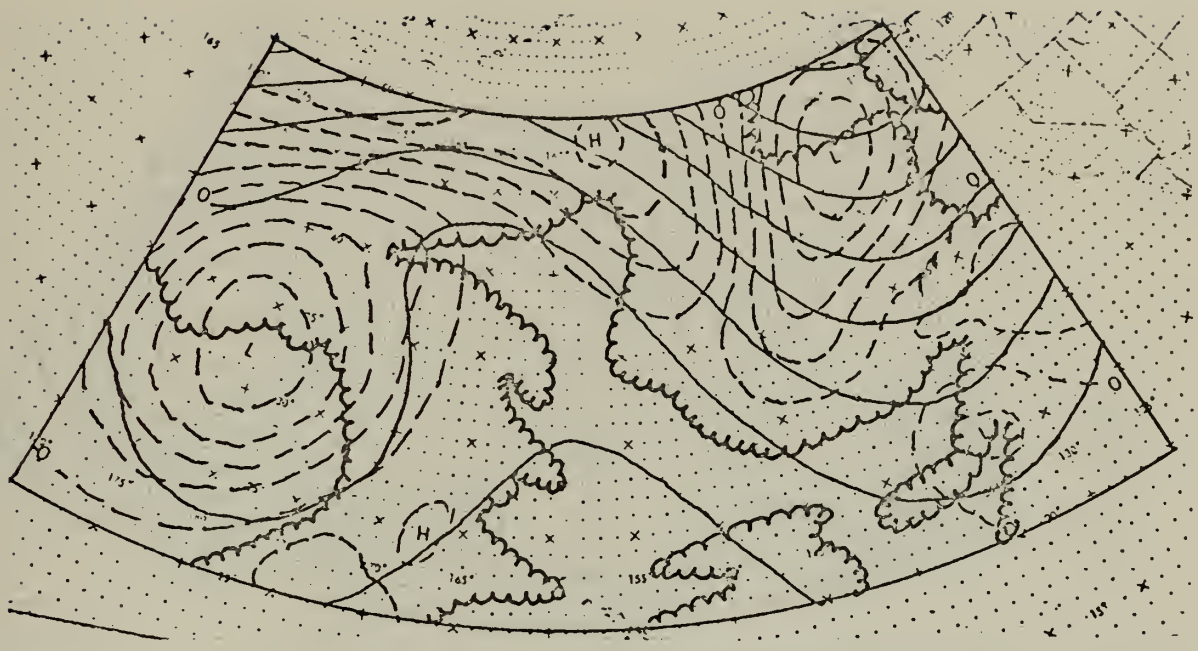

Figure 3. FNWC 500-mb SD (---) and SR (——) analyses, 0000 GMT 10 April 1972, superimposed on the ATS-1 nephanalysis of ≥ 50% cloud cover (2343 GMT 09 April 1972). SD interval: 30 m; zero SD line labeled.

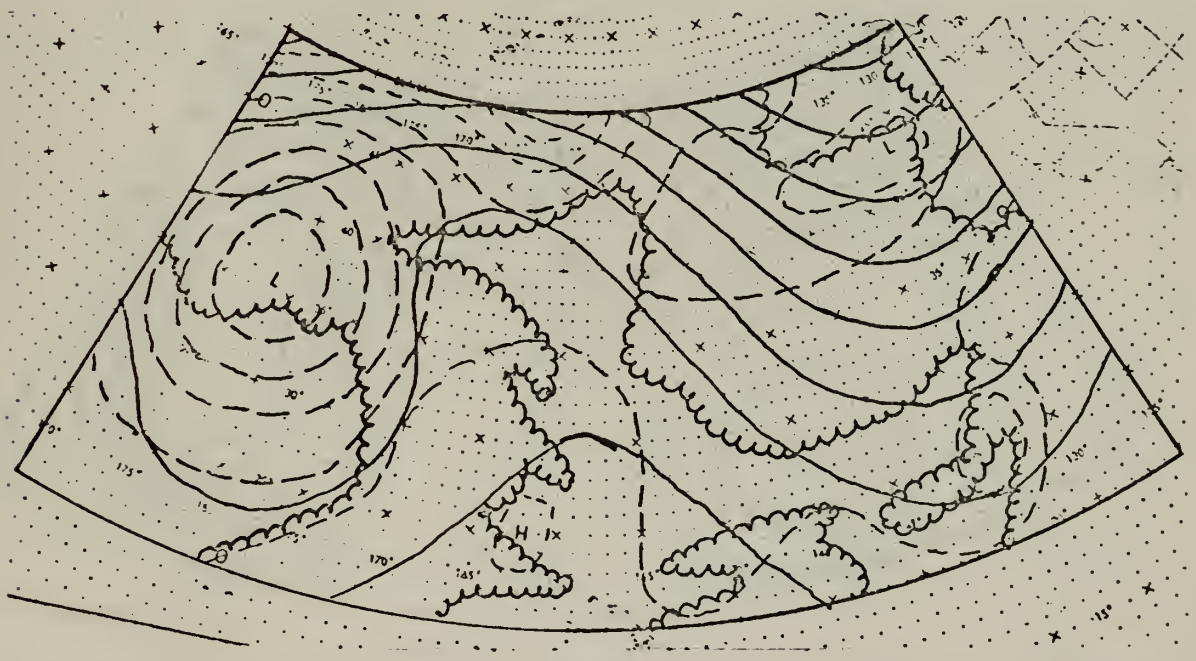

Figure 4. FNWC 500-mb SR (——) and modified SD (---) analyses, 0000 GMT 10 April 1972, superimposed on the ATS-1 nephanalysis of ≥ 50% cloud cover (2343 GMT 09 April 1972). SD interval: 30 m; zero SD line labeled.

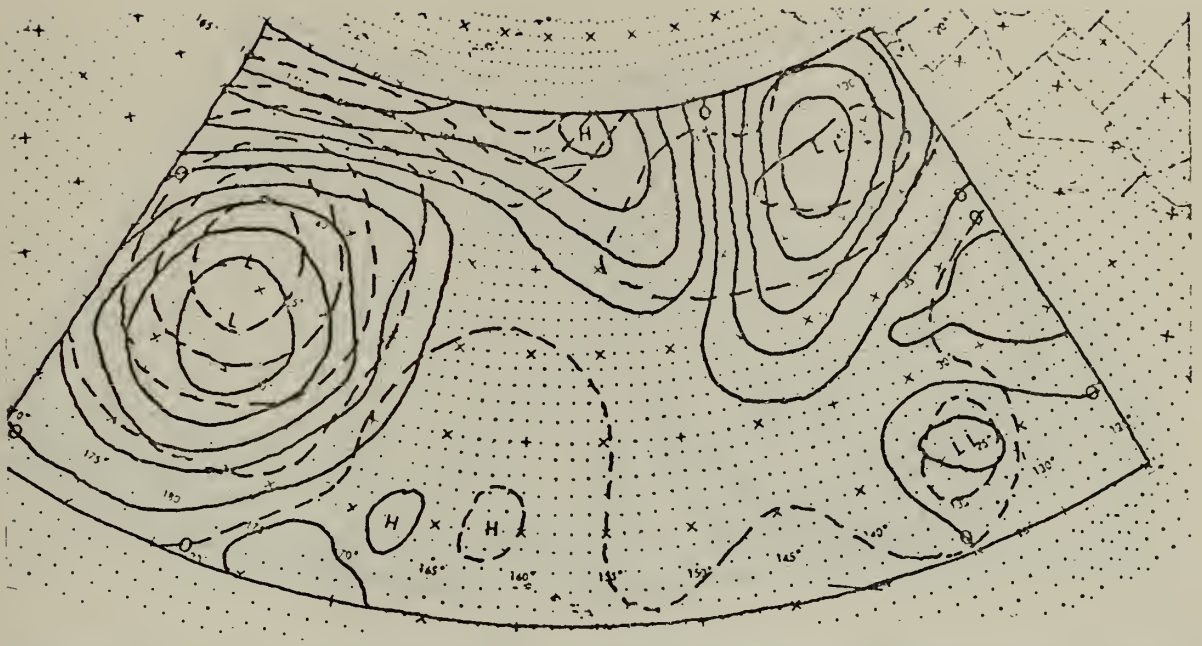

Figure 5. 500-mb FNWC SD (——) and modified FNWC SD (---) analyses, 0000 GMT 10 April 1972: SD interval: 30 m; zero SD line labeled.

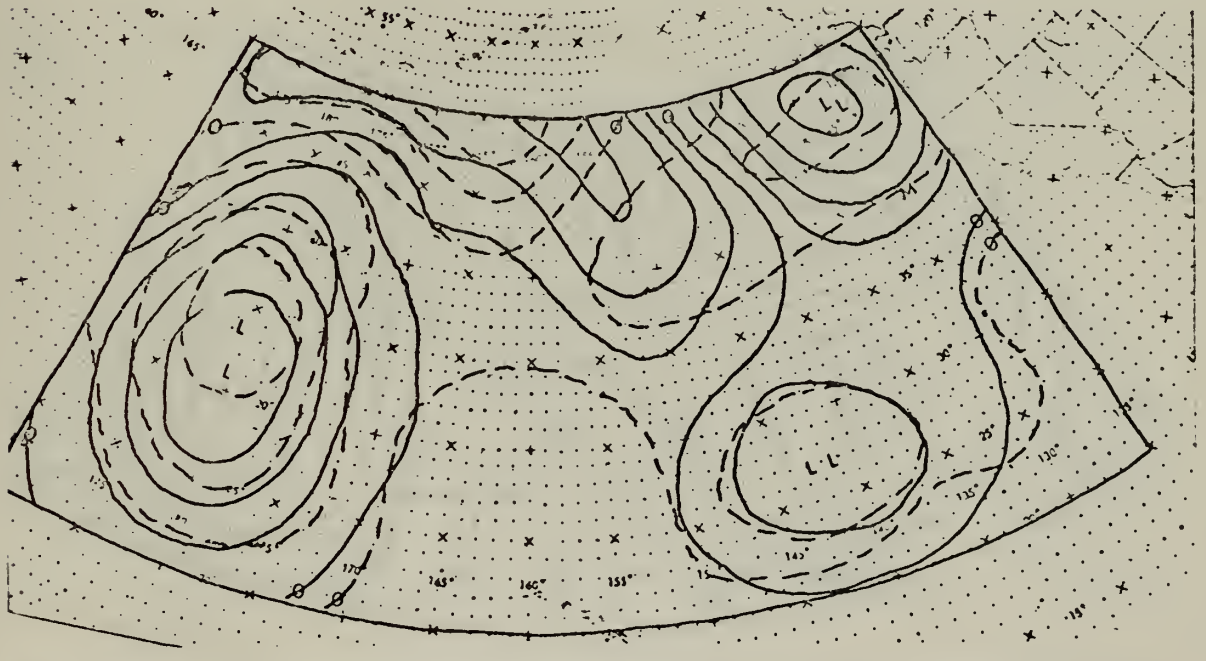

Figure 6. 36-hour 500-mb FNWC SD (——) and modified FNWC SD (---) prognosis, verifying at 0000 GMT 11 April 1972: SD interval: 30 m; zero SD line labeled.

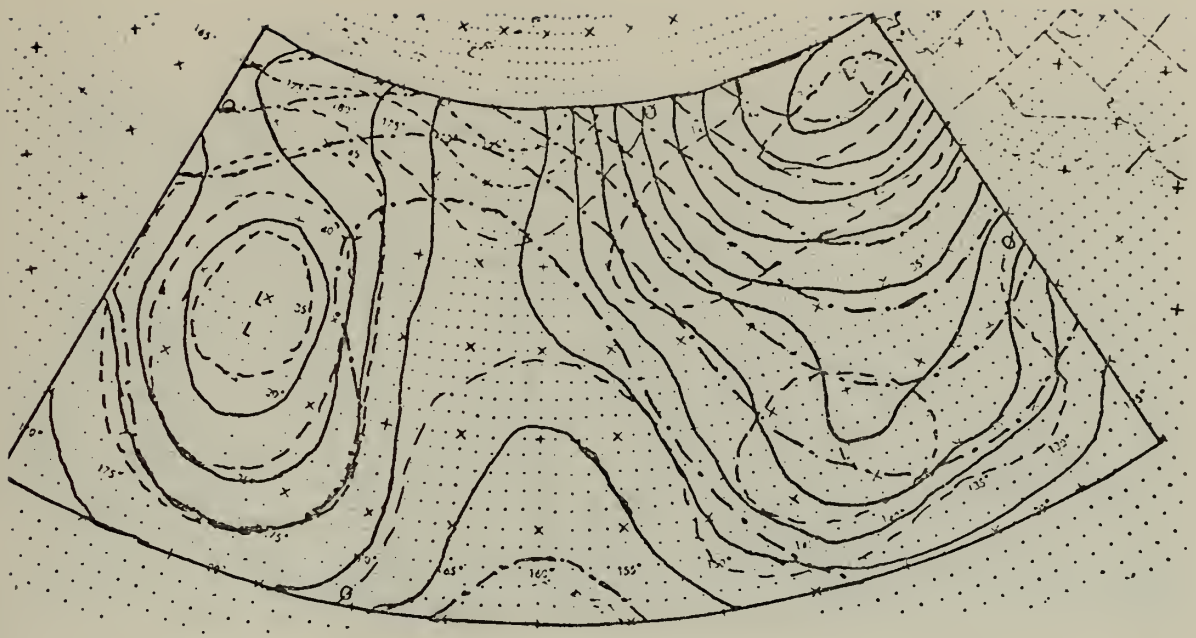

Figure 7. Modified FNWC Z prognosis (——) as derived from the FNWC SR (-•-•) and modified SD (---) prognosis, verifying at 0000 GMT 11 April 1972: SD interval: 30 m; zero SD line labeled.

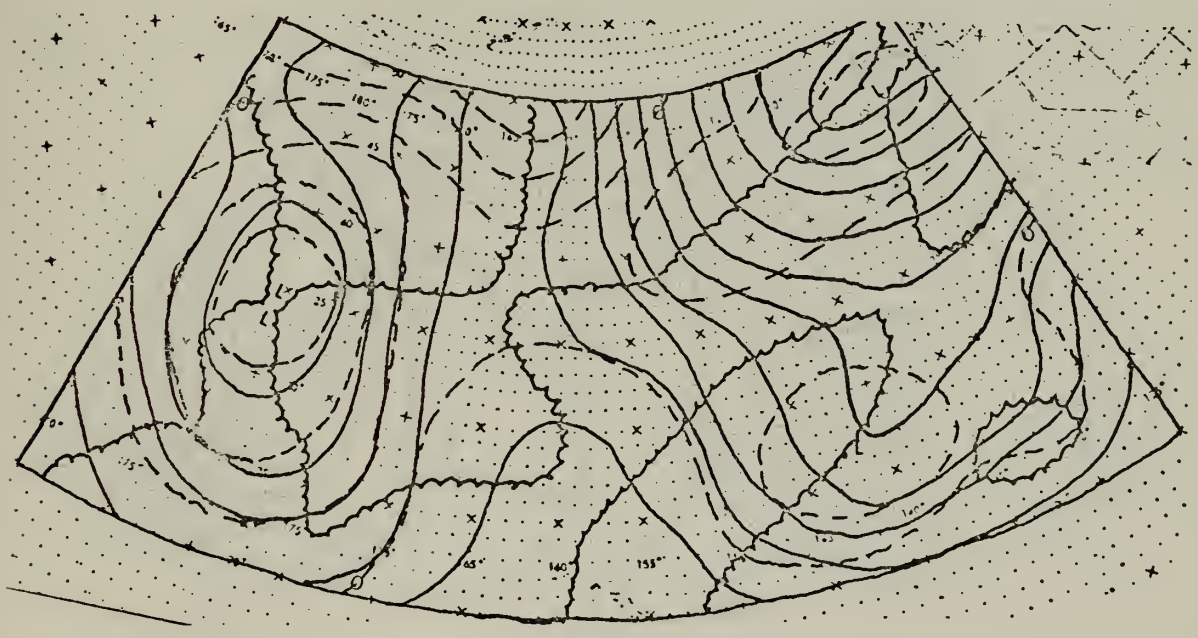

Figure 8. Modified FNWC 500-mb Z (——) and SD (---) prognoses with resulting areas of positive vorticity advection ( ), verifying at 0000 GMT 11 April 1972: SD interval: 30 m; zero SD line labeled.

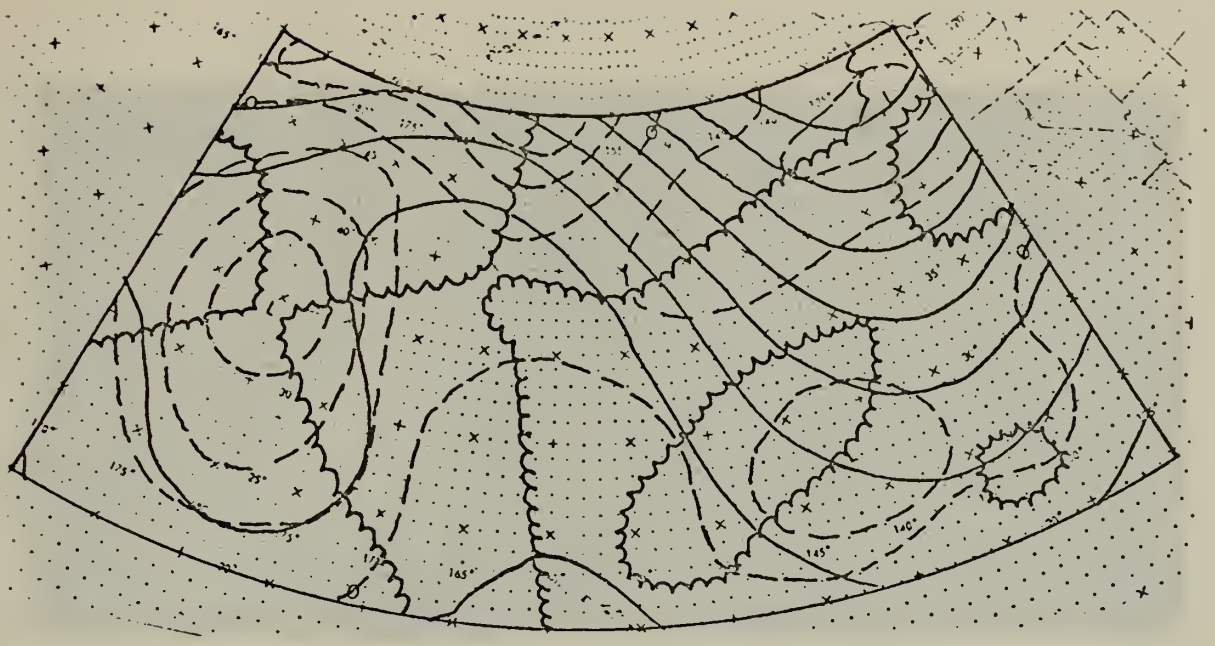

Figure 9. FNWC 500-mb SR (——) and modified SD (---) prognoses with resulting areas of positive vorticity advection ( ), verifying at 0000 GMT 11 April 1972: SD interval: 30 m; zero SD line labeled.

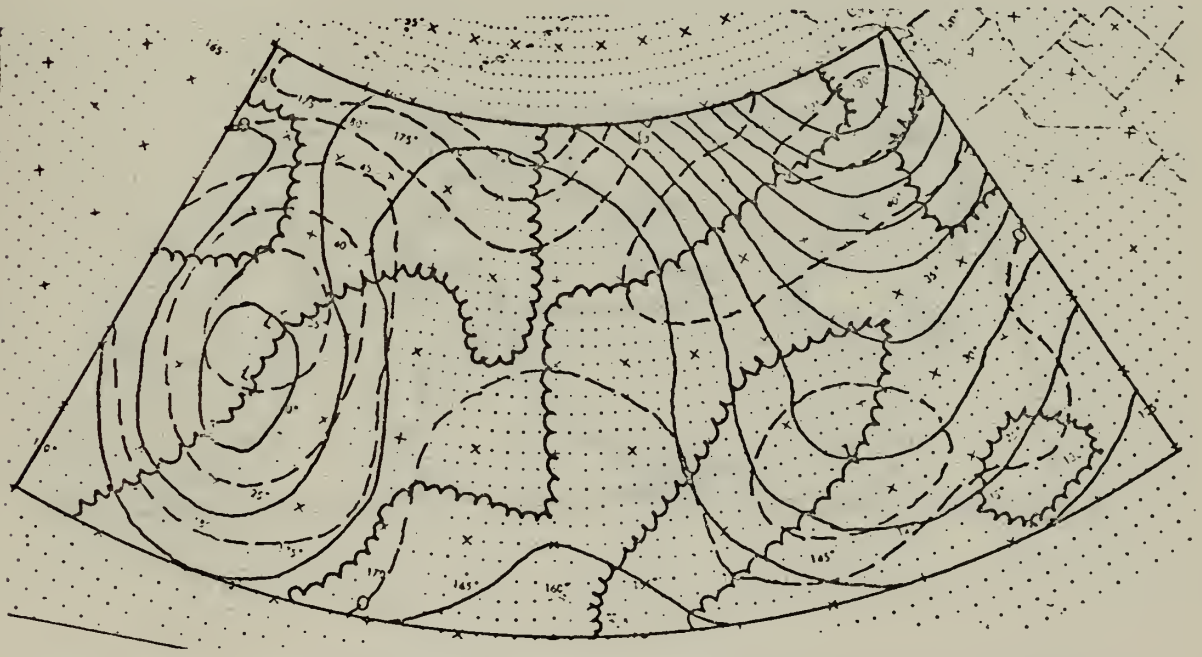

Figure 10. FNWC 500-mb Z (——) and modified SD (---) prognoses with resulting areas of positive vorticity advection ( ), verifying at 0000 GMT 11 April 1972: SD interval: 30 m; zero SD line labeled.

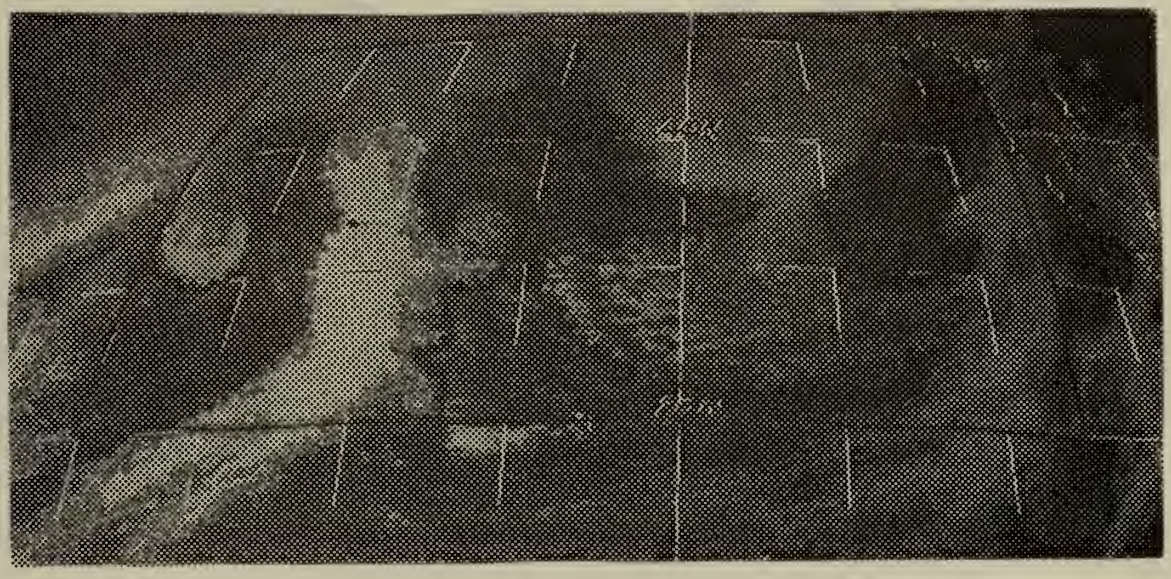

Figure 11. 2358 GMT 10 April 1972 ATS-1 satellite photograph (Subpoint: 2°S). Area of $\geq$ 50% cover bounded by ☁.

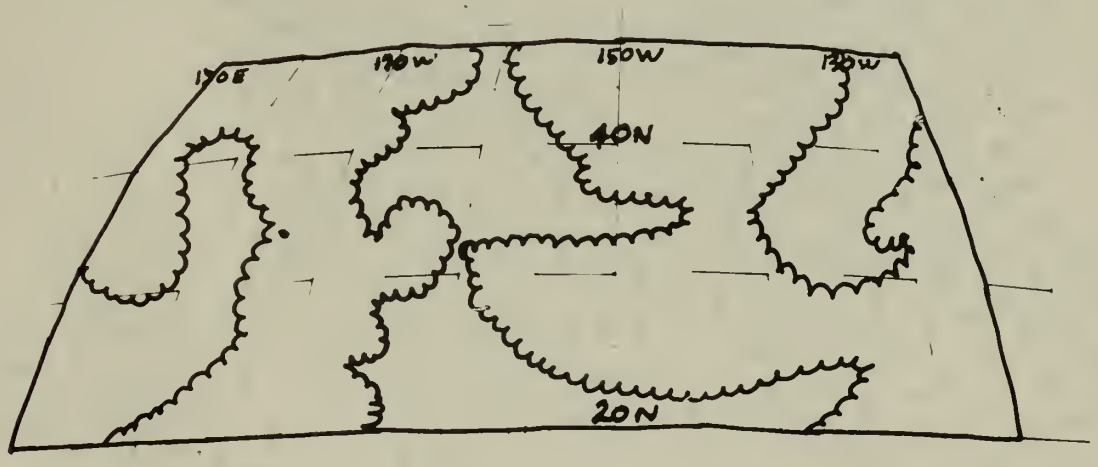

Figure 12. Nephanalysis of ATS-1 satellite photograph (Subpoint: 2°S), 2358 GMT 10 April 1972. Area of $\geq$ 50% cover bounded by ☁ .

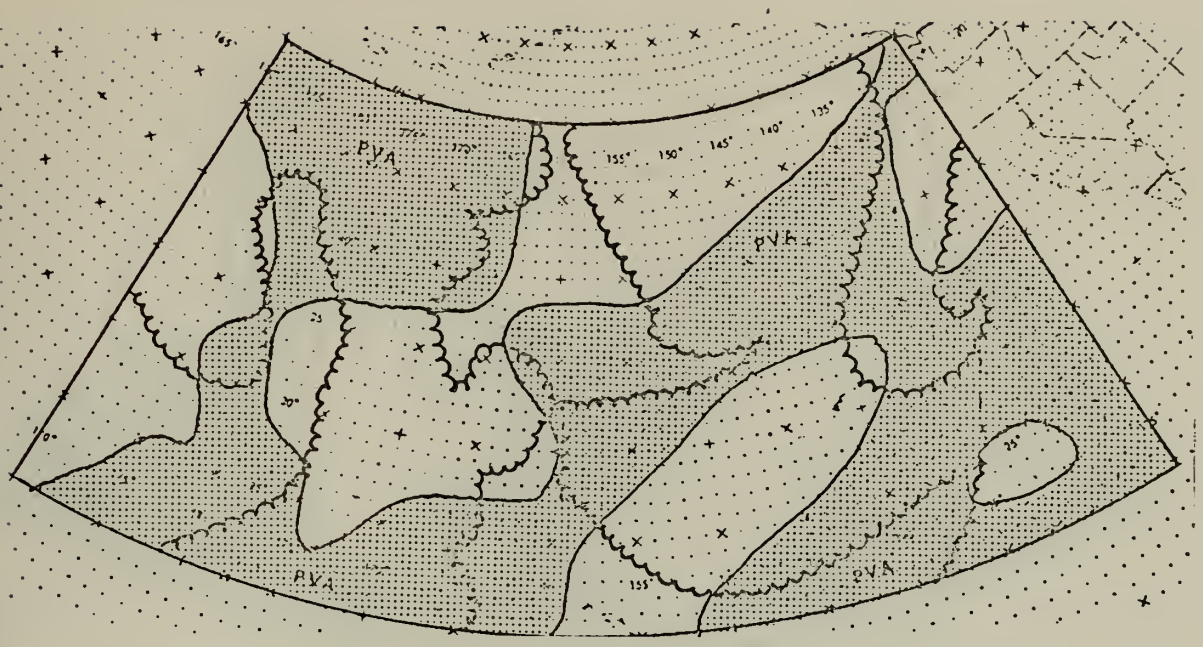

Figure 13. Nephanalysis of ≥ 50% cloud cover from ATS-1 photograph (2358 10 April 1972) ( ), and area of positive vorticity advection, ( ) derived from the modified 36-hour FNWC 500-mb Z prognosis verifying at 0000 GMT 11 April 1972.

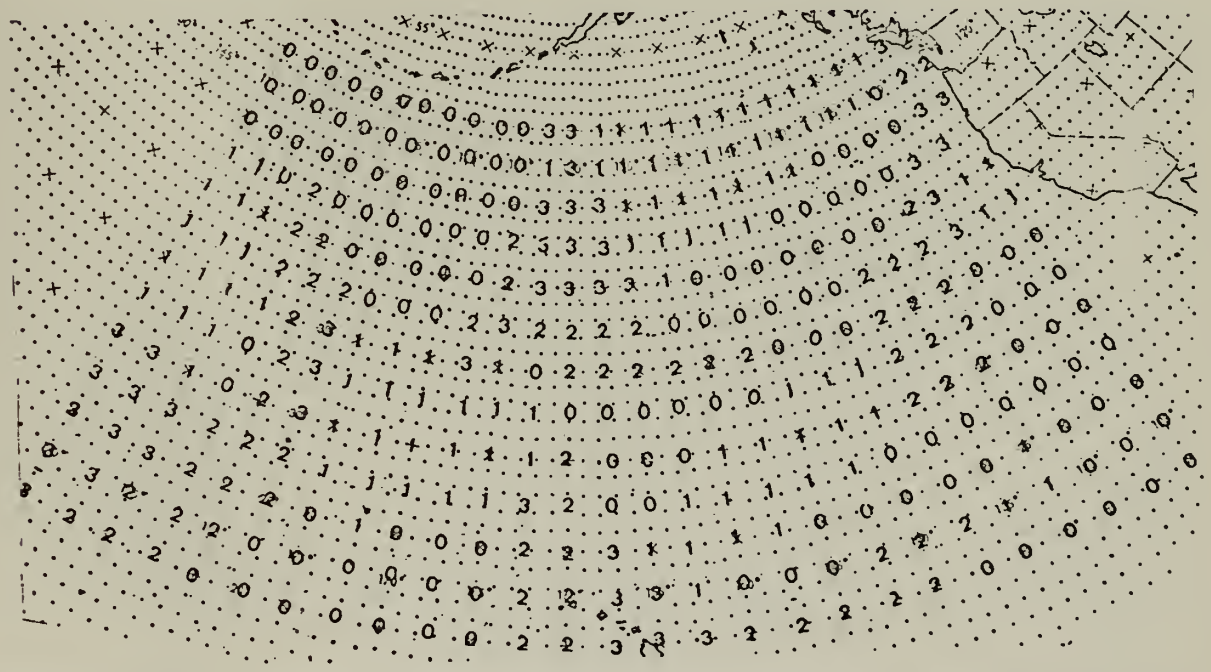

Figure 14. Scoring grid for the cloud forecast based on the modified 36-hour FNWC 500-mb Z prognosis, verifying at 0000 GMT 11 April 1972. Legend: 0-Clouds: forecast and observed-141 points; 1-Clouds: observed but not forecast-101 points; 2-Clouds: forecast but not observed-66 points; 3-Clear: forecast and observed-43 points.

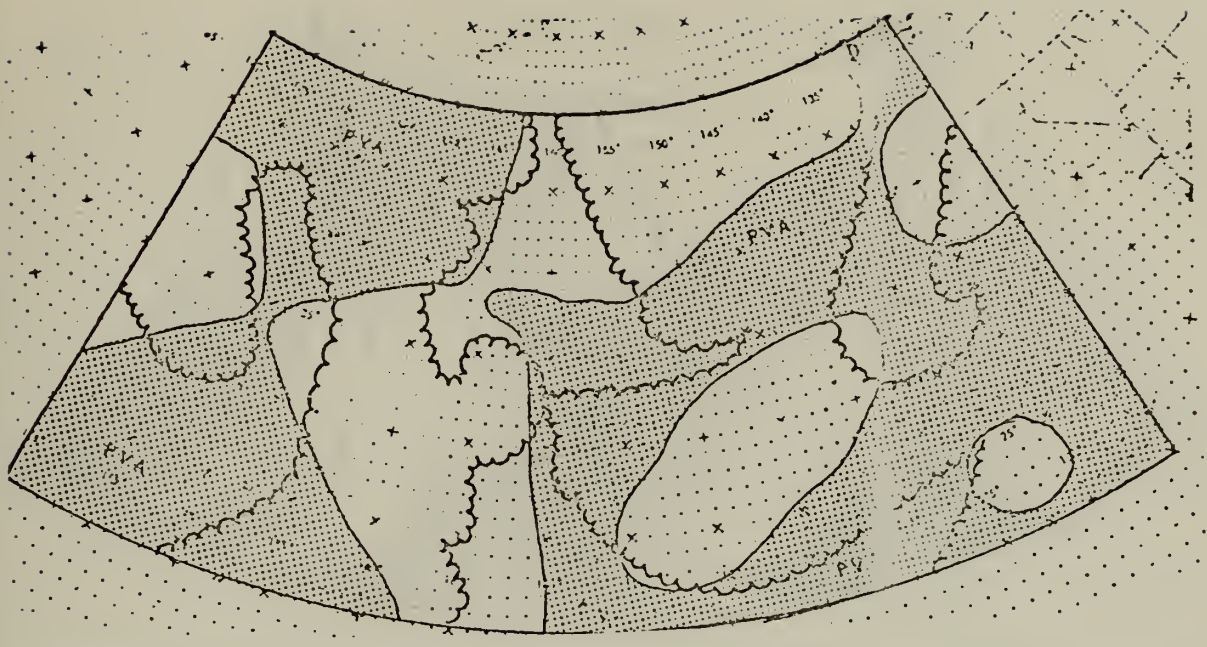

Figure 15. Nephanalysis of ≥ 50% cloud cover from ATS-1 photograph (2358 GMT 10 April 1972) ( ), and area of positive vorticity advection derived from 36-hour FNWC 500-mb SR prognosis verifying at 0000 GMT 11 April 1972.

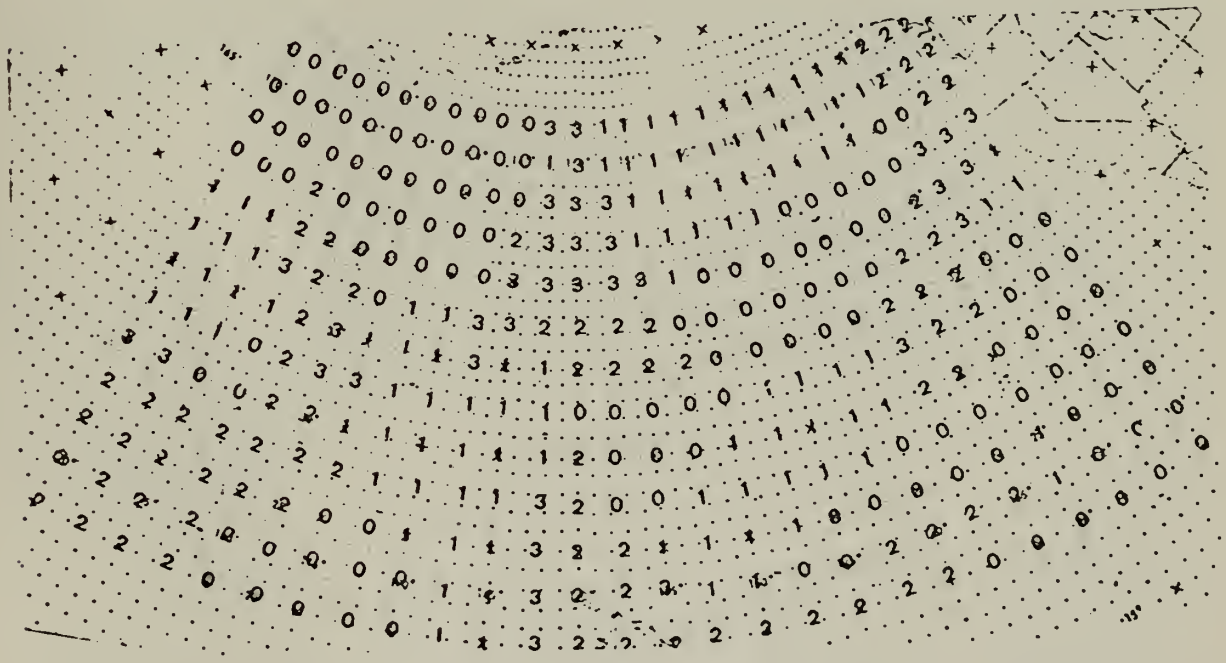

Figure 16. Scoring grid for the cloud forecast based on the modified 36-hour FNWC 500-mb SR prognosis, verifying at 0000 GMT 11 April 1972. Legend: 0-Clouds: forecast and observed-135 points; 1-Clouds: observed but not forecast-105 points; 2-Clouds: forecast but not observed-76 points; 3-Clear: forecast and observed-35 points.

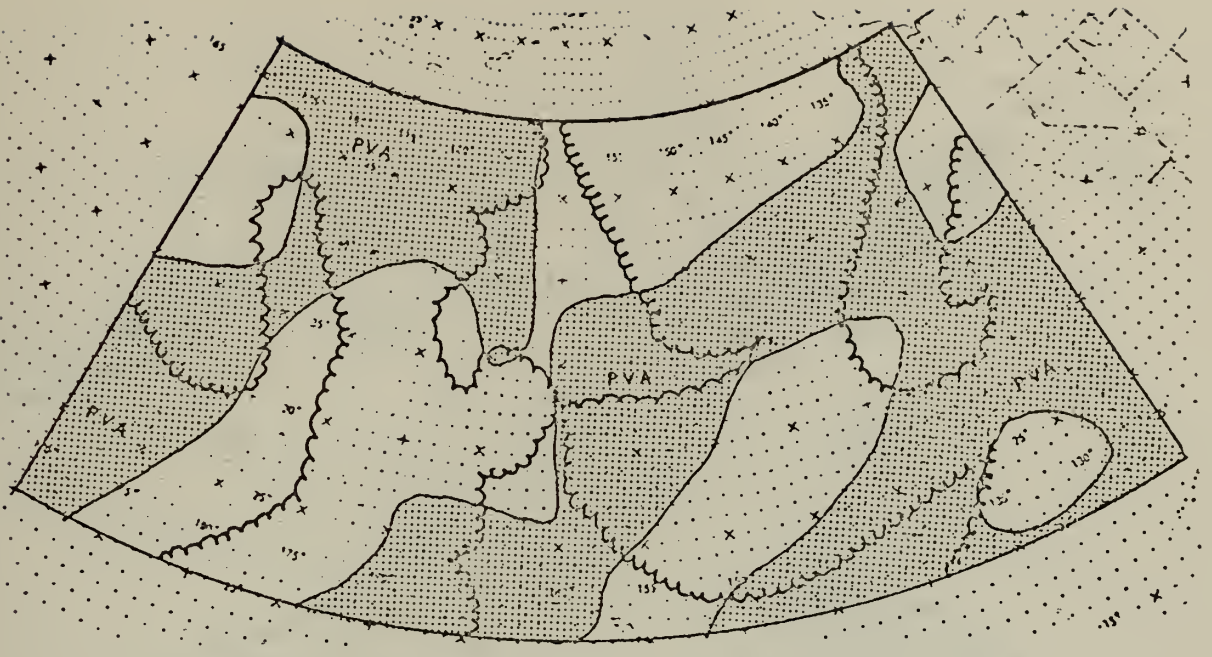

Figure 17. Nephanalysis of ≥ 50% cloud cover from ATS-1 photograph (2358 GMT 10 April 1972) ( ), and area of positive vorticity advection derived from the 36-hour FNWC 500-mb Z prognosis verifying at 0000 GMT 11 April 1972.

Figure 18. Scoring grid for the cloud forecast based on the modified 36-hour FNWC 500-mb Z prognosis, verifying at 0000 GMT 11 April 1972. Legend: 0-Clouds: forecast and observed-127 points; 1-Clouds: observed but not forecast-110 points; 2-Clouds: forecast but not observed-74 points; 3-Clear: forecast and observed-40 points.

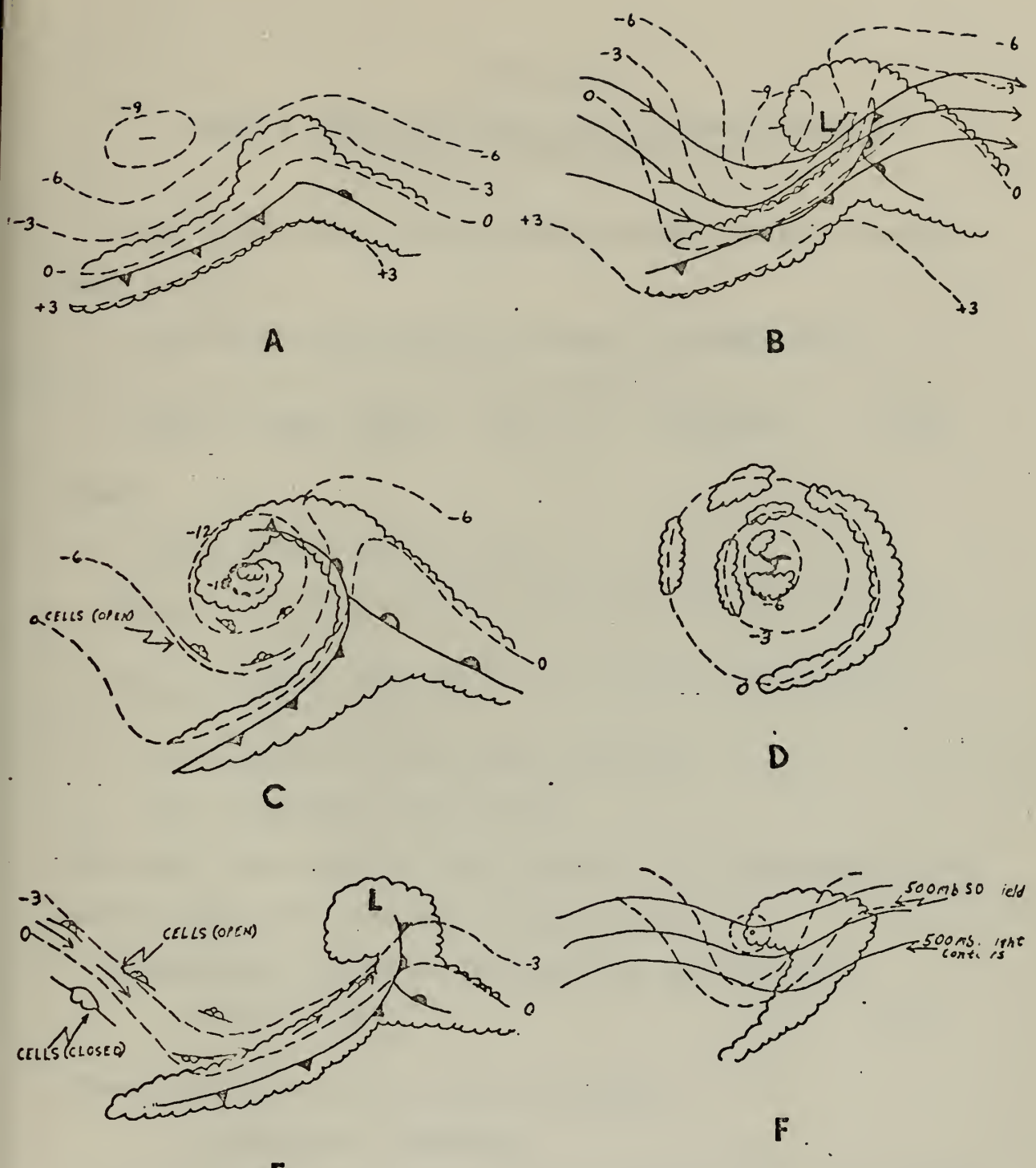

Figure 19. The relationship between cloud patterns and the 500-mb SD field, as presented by Bittner [1] and illustrated by Zeigler [8]: A. Surface wave vs. SD field. B. Occluded system with 500-mb flow and SD field. C. Mature cyclone vs. SD field. D. Dissipating cyclone vs. SD field. E. Polar jet axis and open-celled cumulus vs. zero SD contour. F. SD flow vs. cloud-associated PVA MAX.

APPENDIX A

FNWC'S 500-MB SD FIELD AS AN APPROXIMATION TO THE RELATIVE VORTICITY FIELD

The definitions and discussion below follow closely that in [1].

The 500-mb disturbance component is defined as

$$SD_{500} \equiv Z_{500} - SR_{500} = -\delta S^2 \int_0^{\alpha SD} \nabla^2 Z_{500} d\alpha \qquad (1)$$

where:

Z_{500} = 500-mb height field

SR_{500} = 500-mb residual (mostly wave numbers 1,2,3,4, 5 and 6)

SD_{500} = 500-mb shortwave field (mostly wave numbers 7 and above)

α = degree-of-smoothing parameter

δS = numerical grid length

The right hand side of this equation is a Laplacian of the height field over the smoothing interval α .

Geostrophic relative vorticity is defined as:

$$\zeta = g f^{-1} \nabla^2 Z_{500} \qquad (2)$$

where: g = acceleration due to gravity

f = Coriolis parameter

By substituting Equation (2) into Equation (1), the following relationship is obtained:

$$SD_{500} = -\delta S^2 \, f g^{-1} \int_0^{\alpha SD} \zeta d\alpha \qquad (3)$$

Equation (3) shows that the SD field is about the same as the geostrophic relative vorticity field (with a sign reversal) over the smoothing interval used in the analysis. Thus, for all practical purposes, they can be considered analogous for both analyses and prognoses.

APPENDIX B

SUMMARY OF RULES RELATING CLOUD PATTERNS TO 500-MB SD ANALYSES

Following is a summary of rules relating cloud patterns to the 500-mb analyses [1].

1) The SD zero line should be drawn: (See Figure 19 for a graphical illustration of some of these rules.)
   a) Along the poleward edge of the cloud band associated with the polar front.
   b) Along or just equatorward of the cloud shadow marking the polar jet axis; along or just inside the poleward limit of transverse lines marking the subtropical-jet axis.
   c) Along the line between two major vorticies which are connected by a continuous frontal band.
2) An SD low center should be located:
   a) Five to seven degrees upstream from an open frontal wave, or at the rear edge of the head of a cloud-identified positive vorticity advection maximum (PVA MAX).
   b) Five degrees upstream from the center of a hook-shaped cloud pattern (rapidly developing cyclone).
   c) Within three degrees or less from the center of a complete spiral cloud pattern (mature cyclone).
   d) Directly over or slightly to the east of the center of an open vortex (dissipating cyclone).

e) Over the center of a strong vorticity center in the cold air.

3) An SD trough should be drawn:

a) Through the point where a frontal cloud band forks or fractures.

b) Five to seven degrees upstream from a weak frontal wave (where a closed SD low is not justified).

4) An SD ridge should be drawn:

a) In an occlusion, to coincide with the downstream major cloud boundary or the change from C (cumuliform/stratiform) to MCO (stratiform/cirriform).

b) With anticyclonic curvature near the equatorward edge of a frontal cloud band.

c) With anticyclonic curvature over the peak of a frontal wave pattern.

5) The SD gradient should be maximized:

a) Along the rear edge of a frontal cloud band.

b) In the dry tongue of a hook-shaped vortex.

c) At and poleward of the peak of a frontal wave.

6) SD lines should be drawn:

a) Parallel to lines of cumulus (CELLS OPEN) in the cold-air sector of a cyclonic disturbance.

b) Parallel to cloud lines and bands in a dissipating vortex.

REFERENCES

1. Bittner, F. E., 1971: Forecasting Horizontal Weather Depiction Fields by Satellite and Numerical Products, Naval Air Systems Command, Naval Weapons Engineering Support Activity Detachment (FAMOS), Technical Memo (3-71), Hillcrest Heights, Maryland, 51 pp.

2. Fjortoft, R., 1955: "On the Use of Space-Smoothing in Physical Weather Forecasting." Tellus, v. 7, p. 462-480.

3. Glaes, B. B., 1972: Numerical Reanalysis Through Proportional Differences. Master's Thesis, Naval Postgraduate School, Monterey, California, 57 pp.

4. Holl, M. M., 1963: Scale and Pattern Spectra and Decompositions. Technical Memorandum No. 3, Meteorology International, Inc., Monterey, California, 28 pp.

5. Mantei, T. J. and Workman, C. E., 1971: Experimental Use of Satellite Data in Numerical Analysis and the Effect on a Primitive-Equation Prediction Scheme. Master's Thesis, Naval Postgraduate School, Monterey, California, 119 pp.

6. Nagle, R. E. and Clark, J. R., 1968: An Approach to the SINAP Problem: A Quasi-Objective Method of Incorporating Meteorological Satellite Information in Numerical Weather Analysis. Final Report, Contract No. E-93-67 (N), Meteorology International, Inc., Monterey, California, 142 pp.

7. Nagle, R. E. and Hayden, C. M., 1971: The Use of Satellite-Observed Cloud Patterns in Northern Hemisphere 500-mb Numerical Analysis. National Oceanic and Atmospheric Administration, Technical Report NESS-55, Superintendent of Documents, Washington, D. C., 47 pp.

8. Zeigler, L. E., 1971: Operational Utilization of Weather Satellite Data for Input to Numerical Analysis and Prediction. Master's Thesis, Naval Postgraduate School, Monterey, California, 75 pp.

INITIAL DISTRIBUTION LIST

		No. Copies
1.	Defense Documentation Center Cameron Station Alexandria, Virginia 22314	2
2.	Library, Code 0212 Naval Postgraduate School Monterey, California 93940	2
3.	Department of Meteorology, Code 51 Naval Postgraduate School Monterey, California 93940	2
4.	Lieutenant C. H. Allen, USN Fleet Weather Central Box 113 FPO, San Francisco, California 96610	3
5.	Commander Harry D. Hamilton, USN Fleet Numerical Weather Central Monterey, California 93940	5
6.	Professor R. J. Renard, Code 51Rd Department of Meteorology Naval Postgraduate School Monterey, California 93940	5
7.	Naval Weather Service Command Naval Weather Service Headquarters Washington Naval Yard Washington, D. C. 20390	1
8.	Commanding Officer Fleet Numerical Weather Central Naval Postgraduate School Monterey, California 93940	2
9.	Officer-in-Charge Environmental Prediction Research Facility Monterey, California 93940	2
10.	Mr. Fred Bittner National Environmental Satellite Service National Oceanic and Atmospheric Administration Washington, D. C. 20233	2

Security Classification

DOCUMENT CONTROL DATA - R & D

(Security classification of title, body of abstract and indexing annotation must be entered when the overall report is classified)

ORIGINATING ACTIVITY *(Corporate author)*

Naval Postgraduate School
Monterey, California 93940

2a. REPORT SECURITY CLASSIFICATION

Unclassified

2b. GROUP

REPORT TITLE

Improving 24-Hour Cloud Forecasts By Manually-Modified Numerical Prognoses Based on Satellite Observations

DESCRIPTIVE NOTES *(Type of report and, inclusive dates)*

Master's Thesis; March 1973

AUTHOR(S) *(First name, middle initial, last name)*

Charlie Harvie Allen

REPORT DATE	7a. TOTAL NO. OF PAGES	7b. NO. OF REFS
March 1973	54	8

CONTRACT OR GRANT NO.	9a. ORIGINATOR'S REPORT NUMBER(S)
PROJECT NO.	
	9b. OTHER REPORT NO(S) *(Any other numbers that may be assigned this report)*

DISTRIBUTION STATEMENT

Approved for public release; distribution unlimited.

SUPPLEMENTARY NOTES	12. SPONSORING MILITARY ACTIVITY
	Naval Postgraduate School Monterey, California 93940

ABSTRACT

The results of three quasi-objective techniques for enhancing the accuracy of 24-hour cloud cover forecasts in sparse data areas, using satellite data and numerically-produced analyses and prognoses, are presented. All three of the techniques involve the modification of the analyzed 500-mb relative vorticity, as based on the satellite-observed cloud patterns and the associated changes to the prognostic fields of 500-mb relative vorticity. The final 24-hour cloud-cover forecast is based on the manually-modified relative vorticity pattern and three different advecting currents. These advecting currents are based on the prognostic 500-mb height field, modified and unmodified, and the prognostic 500-mb space mean field. The study was conducted over a large area of the North Pacific Ocean for the period 9 March to 13 April 1972.

DD FORM 1 NOV 68 1473 (PAGE 1)

S/N 0101-807-6811

Security Classification

A-31408

4 KEY WORDS	LINK A		LINK B		LINK C	
	ROLE	WT	ROLE	WT	ROLE	WT
Forecasting						
Cloud Forecasts						
Satellite Observations						
500-mb Prognoses						

Thesis
A37645 Allen
c.1

141993

Improving 24-hour cloud forecasts by manually-modified numerical prognoses based on satellite observations.